

C. Scheuerlein<sup>1</sup>, F. Lackner<sup>1</sup>, F. Savary<sup>1</sup>, B. Rehmer<sup>2</sup>, M. Finn<sup>2</sup>, C. Meyer<sup>2</sup>

<sup>1</sup> European Organization for Nuclear Research (CERN), Geneva, Switzerland

<sup>2</sup> Federal Laboratory for Materials Research and Testing (BAM), Berlin, Germany

**Introduction:** Thermomechanical coil materials properties need to be known for simulating the coil geometry and stress evolution during the reaction heat treatment (HT). We have measured the Young's and shear moduli of the HL-LHC 11 T Nb<sub>3</sub>Sn magnet coil and reaction tool constituents during *in situ* heat cycles with the dynamic methods resonance and impulse excitation. The thermal expansion of the coil components and of a free standing Nb<sub>3</sub>Sn wire were measured by dilation experiments.

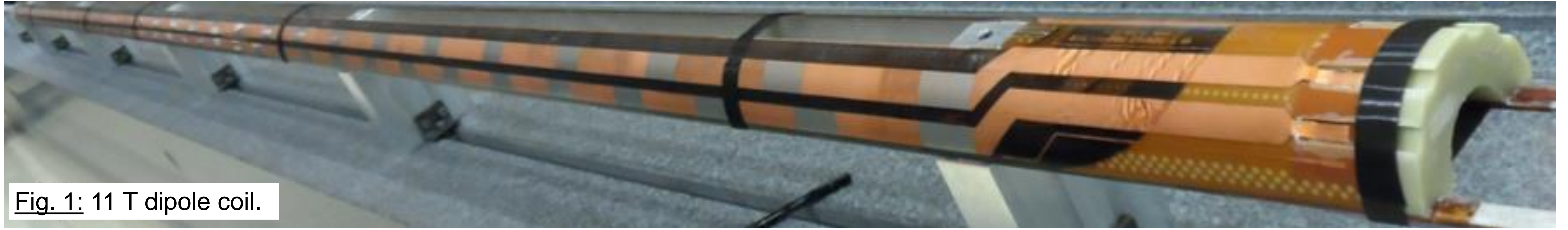


Fig. 1: 11 T dipole coil.

**Thermal expansion:** The unusual thermal expansion behavior of the Nb<sub>3</sub>Sn conductor during first heating, and its mismatch with the thermal expansion of the other coil materials like the DISCUP coil wedges, Ti6Al4V pole wedges and the 316LN stainless steel tooling influence the coil geometry and lead to stress formation in the different components during the thermal cycles. At the end of the Nb<sub>3</sub>Sn reaction the Nb<sub>3</sub>Sn composite wire thermal expansion behavior resembles that of Nb<sub>3</sub>Sn bulk.

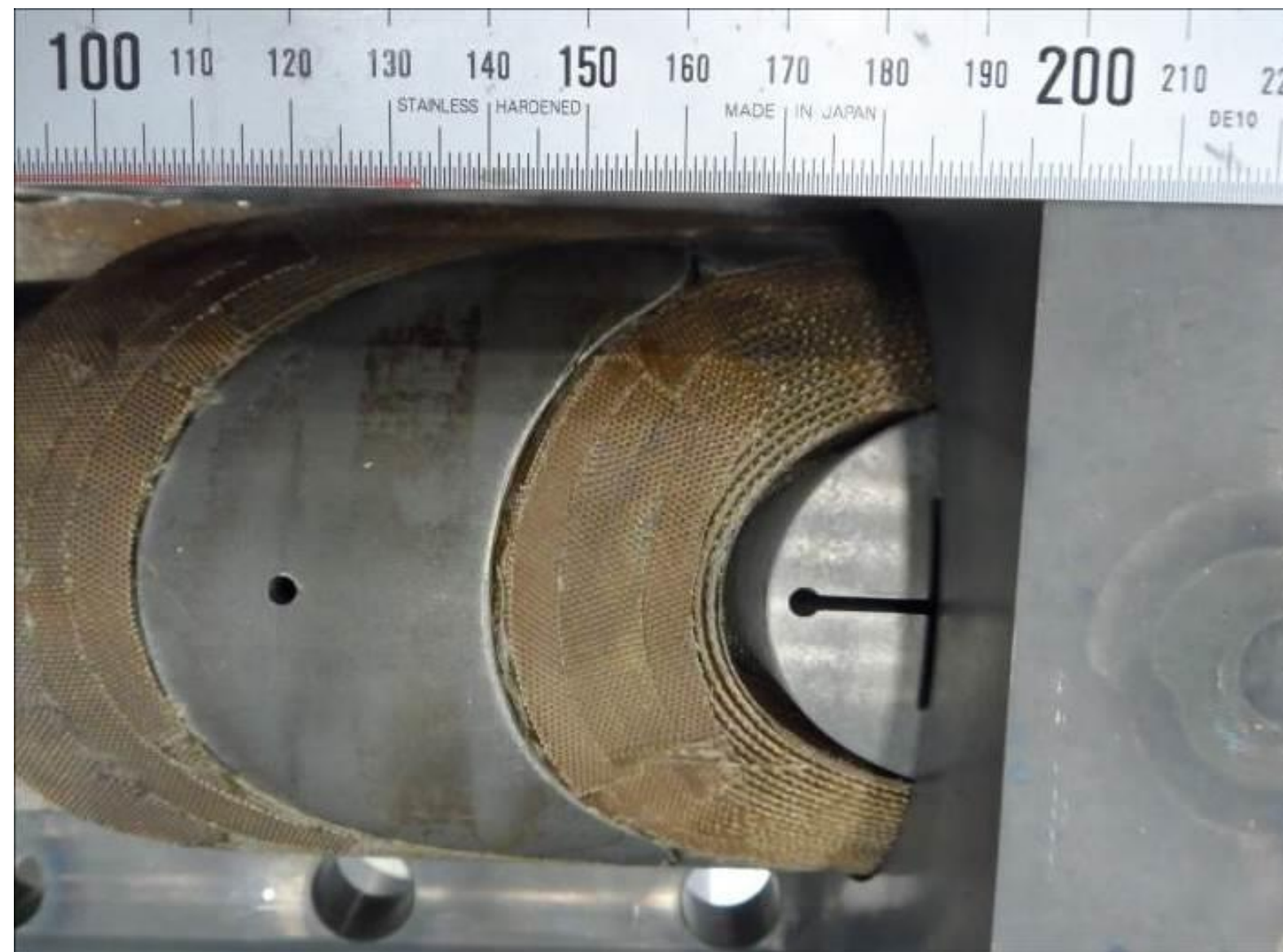


Fig. 2: Reacted 11 T dipole coil pole end inside the 316LN reaction fixture.

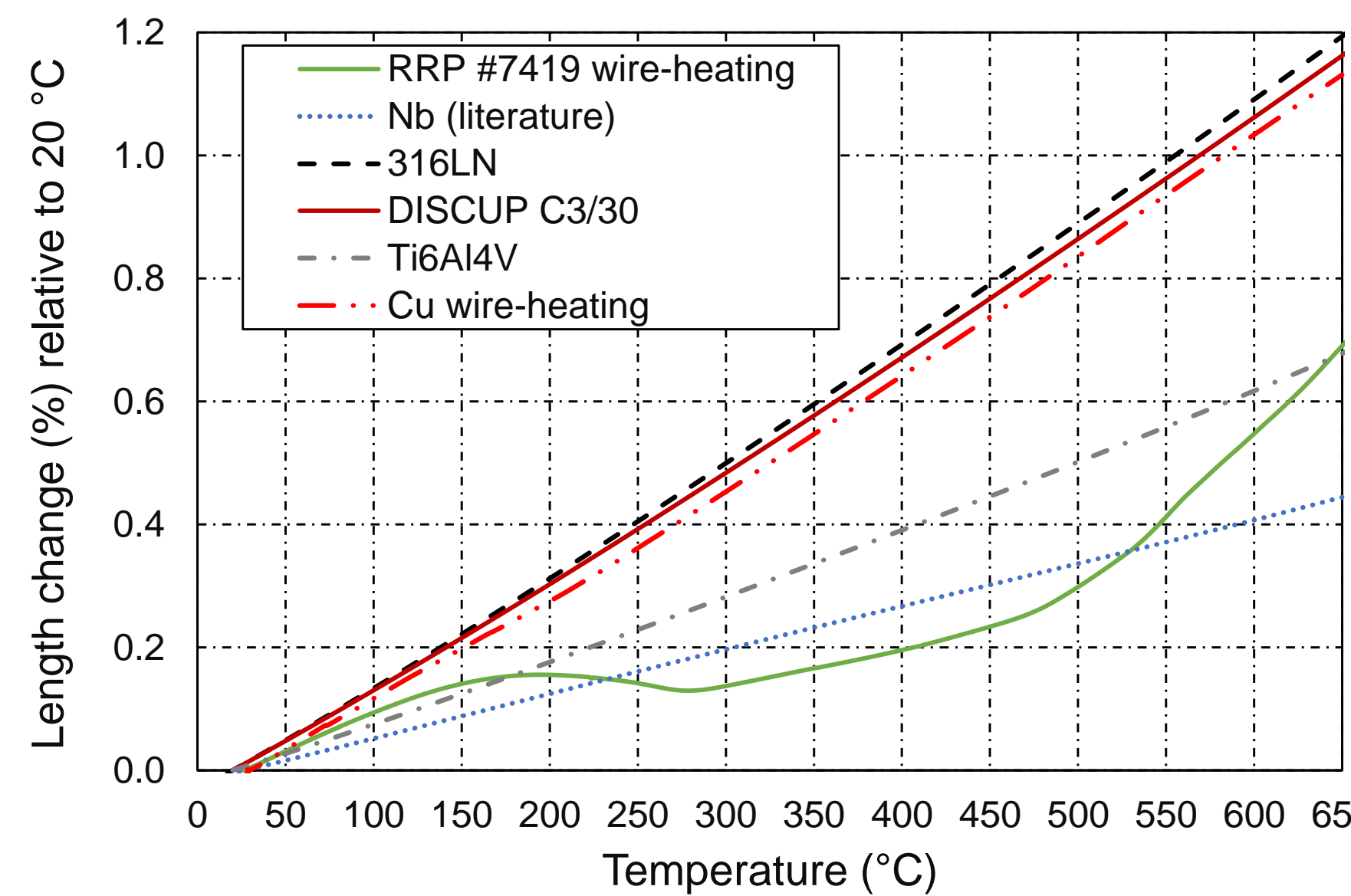


Fig. 3: Relative length change of Nb<sub>3</sub>Sn wire during first heating, DISCUP, Ti6Al4V, and 316LN.

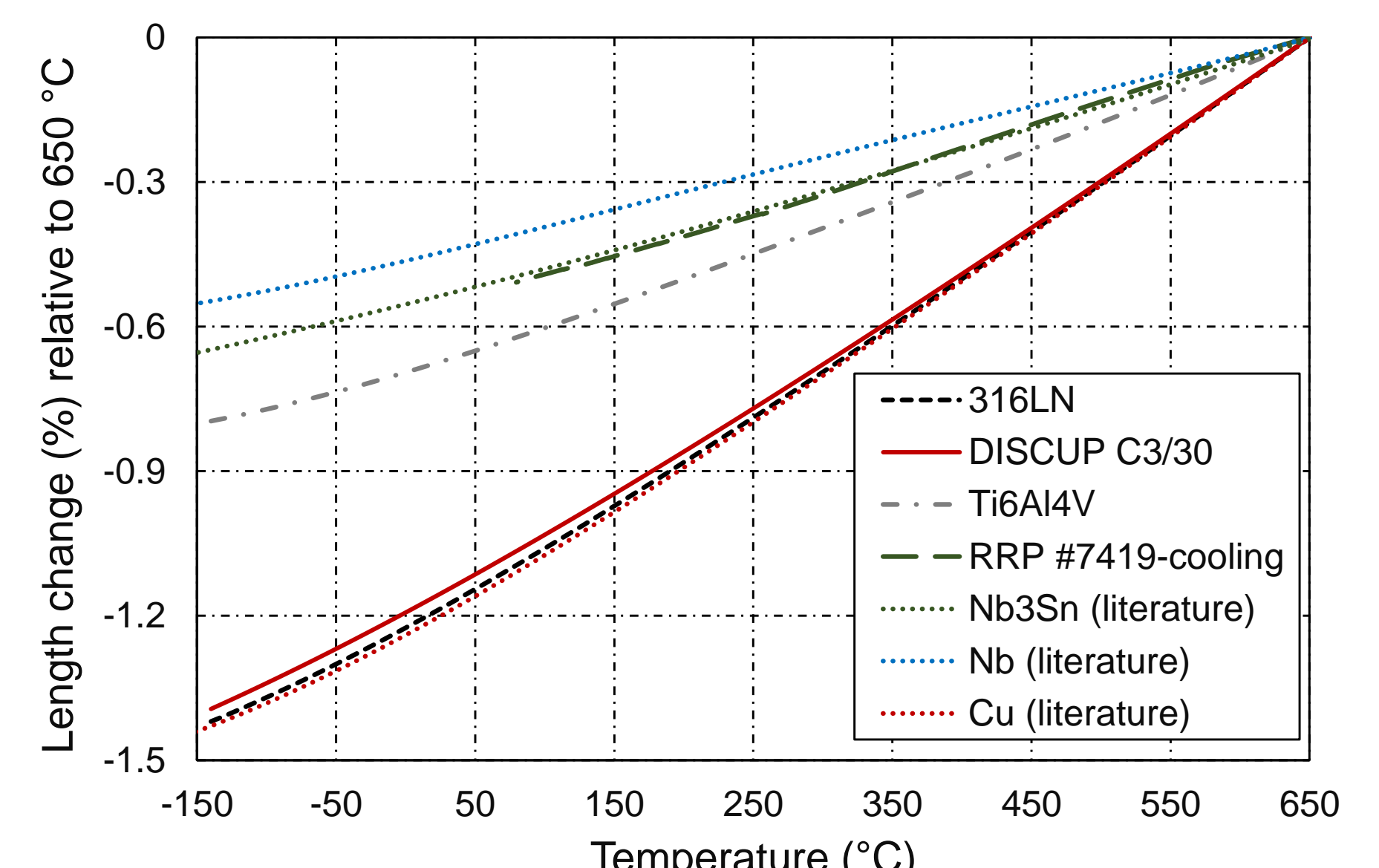


Fig. 4: Relative length change of DISCUP, Ti6Al4V, 316LN and reacted Nb<sub>3</sub>Sn wire during cooling.

**Dynamic Young's and shear moduli:** The evolution of Young's (E) and shear (G) moduli during HT cycles were measured *in situ* during heating in inert gas. E and G are determined from the specimen dimensions (3 mm×9 mm×100 mm), density, and resonance frequencies for bending (Fig. 5) and for torsion, respectively. For isotropic materials Poisson's ratio can be calculated from E and G.

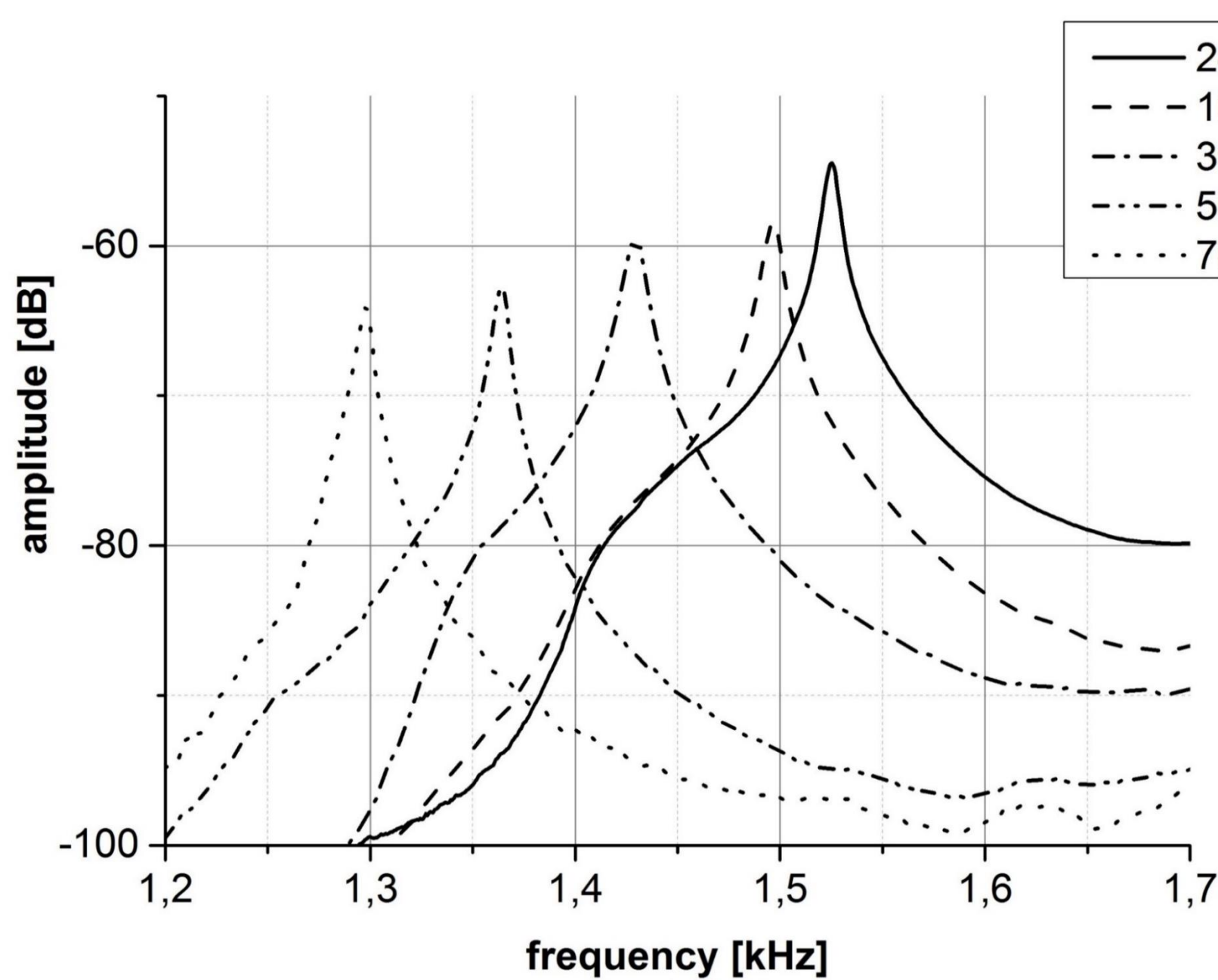


Fig. 5: Resonance peak of the first bending oscillation of the 316LN specimen at different temperatures.

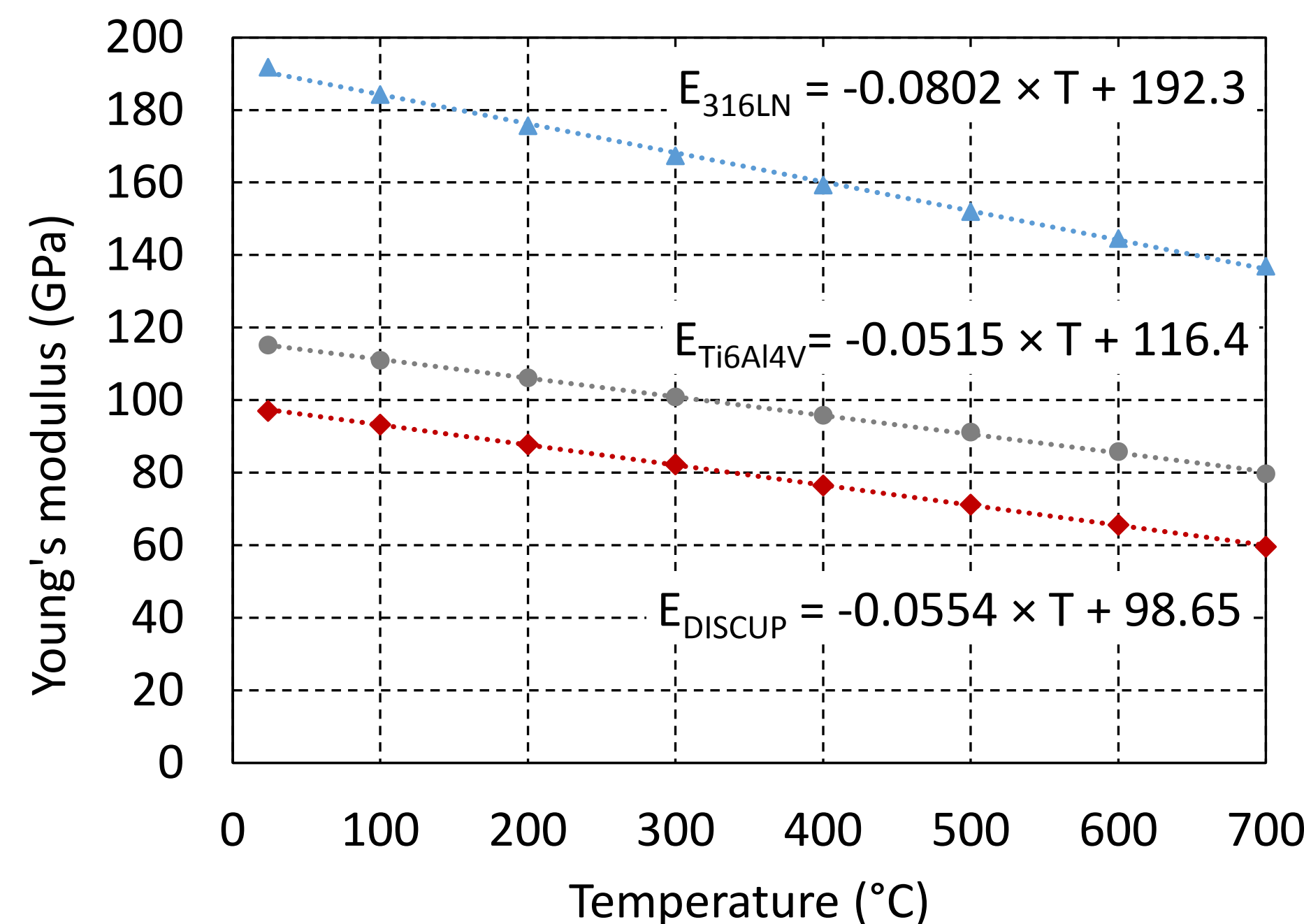


Fig. 6: Young's moduli of DISCUP C3/30, Ti6Al4V and 316LN steel as a function of temperature.

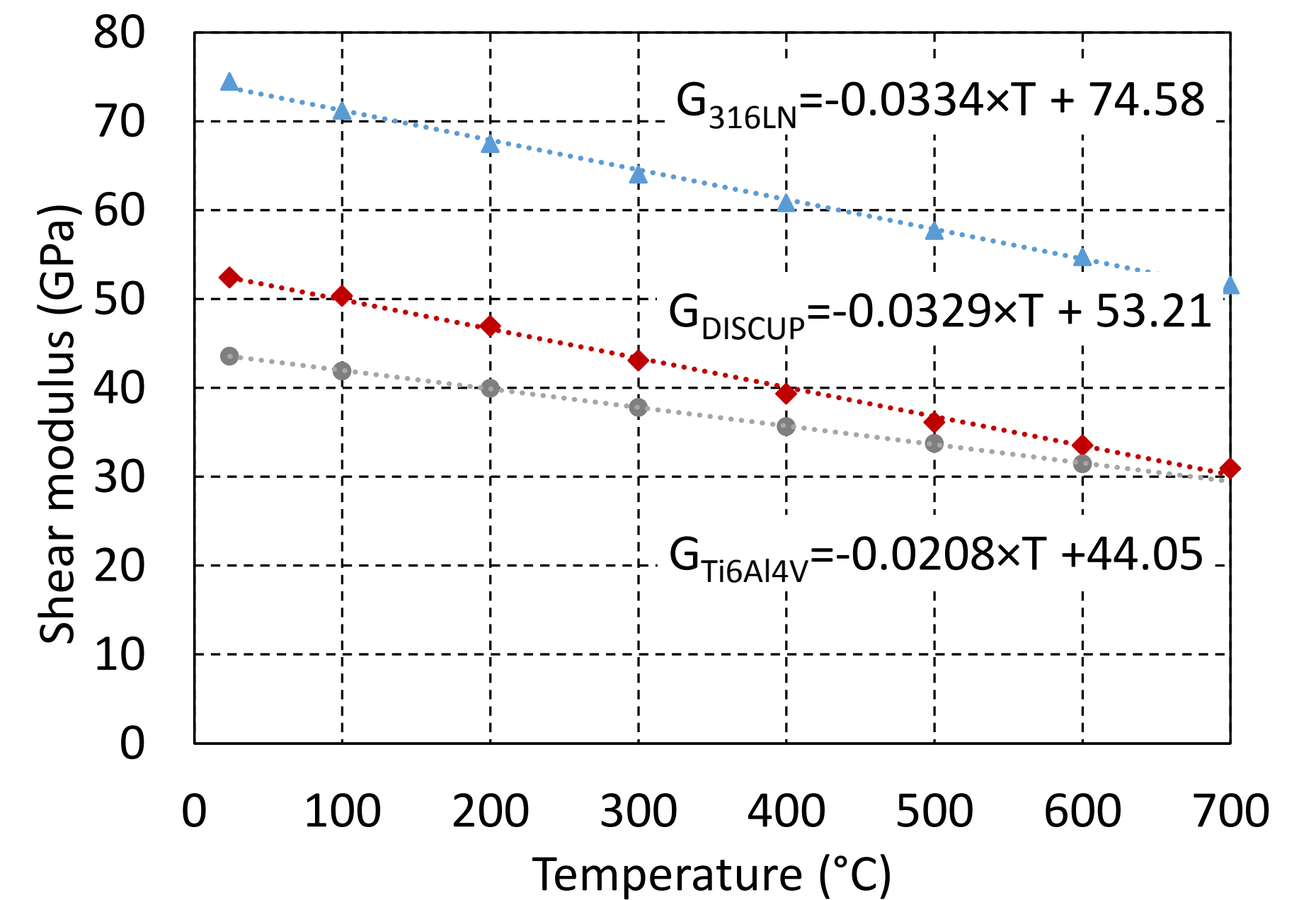


Fig. 7: Shear moduli of DISCUP C3/30, Ti6Al4V and 316LN steel as a function of temperature.

**Static testing:** Stress-strain behavior has been probed by RT uniaxial tensile and compressive testing. Poisson's ratios were determined with the set-up shown in Fig. 4 ( $\nu_{\text{DISCUP}}=0.43$  and  $\nu_{\text{Ti6Al4V-static}}=0.32$ ).



Fig. 8: Set-up with extensometers for axial and for radial strain measurement.

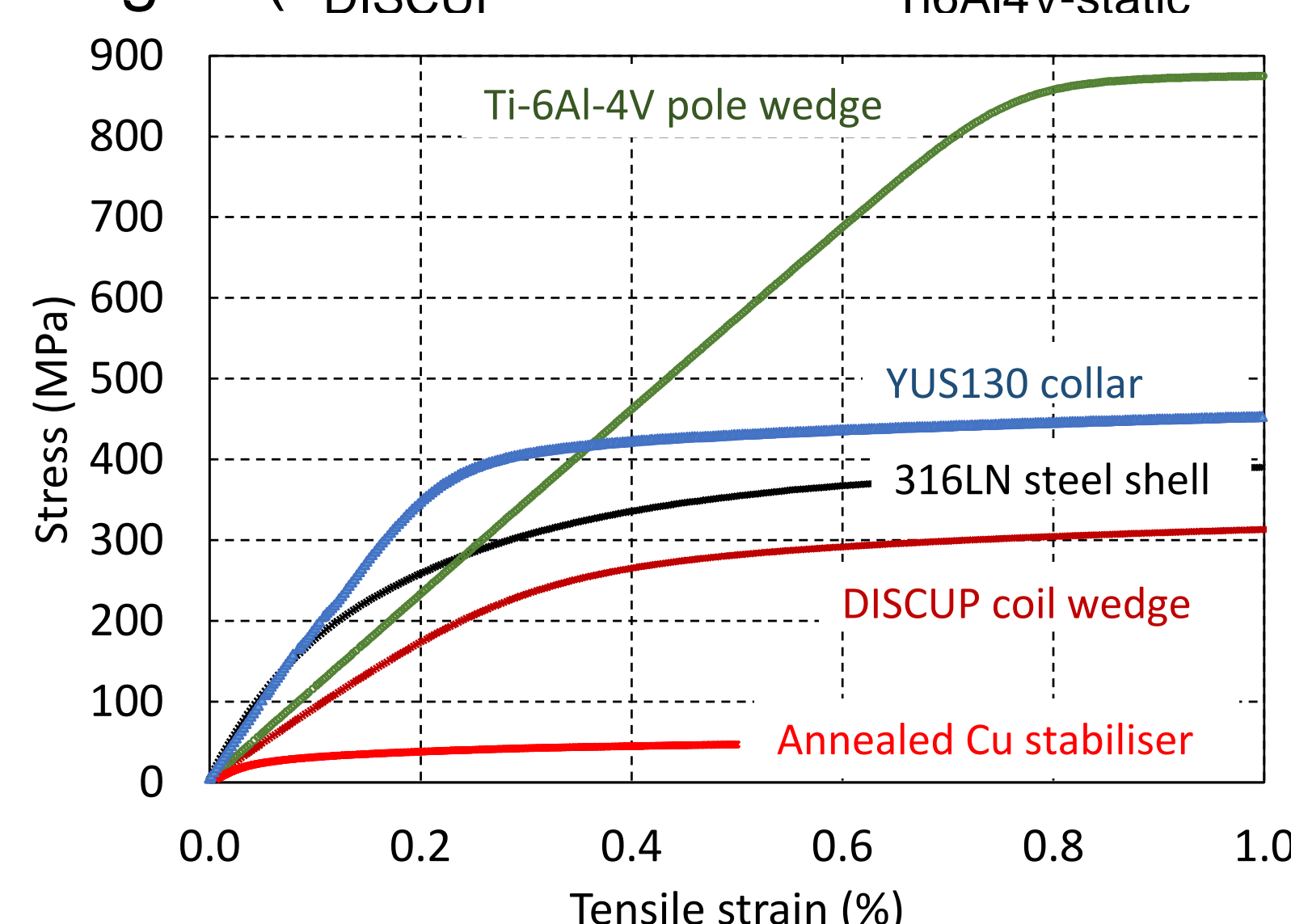


Fig. 9: Comparison of RT stress-strain curves of different coil materials.

**Reference:** C. Scheuerlein, F. Lackner, F. Savary, B. Rehmer, M. Finn, P. Uhlemann, "Mechanical properties of the HL-LHC 11 Tesla Nb<sub>3</sub>Sn magnet constituent materials", IEEE Trans. Appl. Supercond., 27(4), (2017), 4003007.

